*31st EPS Conference on Plasma Phys. London, 28 June - 2 July 2004 ECA Vol.**28G**, P-1.159 (2004)*

Quantitative forward modelling of neutron emission to derive transport coefficients of tritium in JET, including error propagation through to transport parameters

A D Whiteford[1], K-D Zastrow[2], M Adams[2], L Bertalot[3], S Conroy[4], M G O'Mullane[1], S Popovichev[2], H P Summers[1], A Zabolotsky[5] and JET EFDA contributors*

[1]*University of Strathclyde, Glasgow, UK*

[2]*Euratom/UKAEA Fusion Association, Culham Science Centre, Abingdon, UK*

[3]*Associazione EURATOM-ENEA sulla Fusione, Frascati, Italy*

[4]*Uppsala University, EURATOM-VR Asociation, Uppsala, Sweden*

[5]*CRPP, Association EURATOM-Confédération Suisse, Lausanne, Switzerland*

**See annex of J Pamela et al Fusion Energy 2002 (Proc. 19th. Int. Conf. Lyon 2002)*

1 Introduction

In the recent trace tritium experiments at JET, neutron cameras were the only diagnostics which could be used to study adequately the transport of tritium as a function of space and time. Direct confrontation is made between the measured neutron camera data and a forward model of 14MeV and 2.5MeV neutron detectors in order to derive the transport coefficients.

The analysis method for tritium transport is presented, including a discussion of the error propagation techniques used in determining transport coefficients. More details of the results and meaning of this analysis can be found in [1,2]. See also [3] for a specific utilisation on the study of neoclassical tearing modes. Tritium was introduced by both gas puffing and high energy neutral beams ('beam blips') — see [1] for more details.

We show that it is possible to obtain a quantitative uncertainty on derived tritium transport coefficients from measured data. This analysis method can also be applied to other measurements and species. The practical implementation of this work is the computer code UTC[4].

2 Neutron emission

The JET neutron profile monitor measures 2.5 and 14 MeV neutrons along nineteen lines of sight, ten horizontal and nine vertical (see figure 1). In addition to this, global 2.5 and 14 MeV yields are measured. The neutrons are produced partly from fusion reactions of the thermal plasma ions and (often dominantly) by collisions between fast deuterium ions from neutral beam injection (NBI) and the thermal plasma.

The emissivities to model the emission come from TRANSP (see [2]) — a correct description of the poloidal asymmetry of the fast deuterium ions distribution from NBI is necessary in order to model the vertical lines of sight.

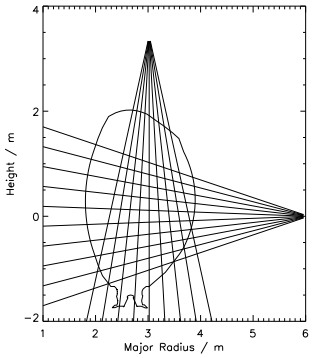

Figure 1: Lines of sight of the JET neutron profile monitor.

Neutrons scatter within the vessel and detector systems, two distinct types are considered:

- Forward scattering — where a neutron emitted along a particular line of sight is deflected to another detector either in the vessel or detection system.
- Back scattering — where a neutron emitted in an arbitrary direction is reflected from the walls of the vessel into a detector.

In addition, some D–T neutrons will register 2.5MeV counts and hence be counted as D–D neutrons due to both detector effects and energy downscatter.

Neutron calibration[5] and MCNP calculations[6] for scattering provide the following data:

- S_N^F — 19×19 matrix with data of how a type N (DD or DT) neutron in one line of sight scatters into the line of sight of another detector,
- S_N^B — 19 element vector with data on how globally emitted type N (DD or DT) neutrons are back scattered into a detector,
- $\varepsilon_{N\to E}$ — Efficiency of a type N neutron (DD or DT) registering a count of energy E ($2.5\mathrm{MeV}$ or $14\mathrm{MeV}$).

We define $L_{2.5}$ to be a vector containing the emission of the neutrons along a particular line of sight, with the index of the vector corresponding to a given detector and $R_{2.5}$ to be the modelled 'recorded' counts of the detector (similarly for L_{14} and R_{14}). With $\Gamma_{2.5}$ and Γ_{14} being modelled global neutron yields we obtain:

$$\begin{bmatrix} \begin{bmatrix} R_{2.5} \end{bmatrix} \\ \begin{bmatrix} R_{14} \end{bmatrix} \end{bmatrix} = \begin{bmatrix} \begin{bmatrix} A \end{bmatrix} & \begin{bmatrix} B \end{bmatrix} & \begin{bmatrix} E \end{bmatrix} & \begin{bmatrix} F \end{bmatrix} \\ \begin{bmatrix} C \end{bmatrix} & \begin{bmatrix} D \end{bmatrix} & \begin{bmatrix} G \end{bmatrix} & \begin{bmatrix} H \end{bmatrix} \end{bmatrix} \begin{bmatrix} \begin{bmatrix} L_{2.5} \end{bmatrix} \\ \begin{bmatrix} L_{14} \end{bmatrix} \\ \Gamma_{2.5} \\ \Gamma_{14} \end{bmatrix},$$

where the sub-matrices A-D represent how the line of sight modelled quantities influence the detection, and the sub-vectors E-H influence how the modelled global neutron yield influences the detectors, these are defined from the calibration/MCNP calculations as:

$$\begin{array}{l|l} A(n,m) = S^F_{\mathrm{DD}}(n,m)\,\varepsilon_{\mathrm{DD}\to 2.5\mathrm{MeV}}(n) & E(n) = S^B_{\mathrm{DD}}(n)\,\varepsilon_{\mathrm{DD}\to 2.5\mathrm{MeV}}(n) \\ B(n,m) = S^F_{\mathrm{DT}}(n,m)\,\varepsilon_{\mathrm{DT}\to 2.5\mathrm{MeV}}(n) & F(n) = S^B_{\mathrm{DT}}(n)\,\varepsilon_{\mathrm{DT}\to 2.5\mathrm{MeV}}(n) \\ C(n,m) = S^F_{\mathrm{DT}}(n,m)\,\varepsilon_{\mathrm{DD}\to 14\mathrm{MeV}}(n) & G(n) = S^B_{\mathrm{DD}}(n)\,\varepsilon_{\mathrm{DD}\to 14\mathrm{MeV}}(n) \\ D(n,m) = S^F_{\mathrm{DT}}(n,m)\,\varepsilon_{\mathrm{DT}\to 14\mathrm{MeV}}(n) & H(n) = S^B_{\mathrm{DT}}(n)\,\varepsilon_{\mathrm{DT}\to 14\mathrm{MeV}}(n) \end{array}$$

3 Transport and influx model

We use SANCO to propagate the equations

$$\frac{\partial n_z}{\partial t} = -\frac{1}{\frac{\partial V}{\partial \psi}}\frac{\partial}{\partial \psi}\left(\frac{\partial V}{\partial \psi}\left\langle \Gamma\psi\right\rangle\right) + \mathrm{Sources} - \mathrm{Sinks} \quad ; \quad \Gamma = -D\left\langle |\nabla\psi|^2\right\rangle \frac{\partial n_z}{\partial \psi} + v\left\langle |\nabla\psi|\right\rangle n_z$$

giving tritium density (n_z) as a function of space and time, from this we forward model neutron counts (see section 2). D, v/D and our influx model are parameterised and used as fit parameters against the measured neutron counts and with a decay time measured from a beam blip shot[2] by fitting an exponential decay to total tritium content. D and v/D are specified/fitted at discrete points in space and time with linear interpolation between points.

Our influx model takes into account the gas puff and wall recycling via a four parameter model to describe (i) gas influx, (ii) tritium going to the wall directly from the puff, (iii) tritium entering from the wall and (iv) recycling in the scrape off layer. Sensitivity studies[2] showed that core transport parameters are relatively (within their error bars) insensitive to the unknowns in the influx model.

4 Fitting and error propagation

Levenberg-Marquardt fitting is employed; we take take numerical derivatives and then finds an iterative solution of $M\mathbf{\Delta p} = \mathbf{b}$. $\mathbf{\Delta p}$ are the 'suggested' adjustments of the free parameters and for the case of only statistical errors, M and $\mathbf{b}$ are

$$M_{ij} = \sum_{n=1}^{N} \frac{\partial f_n}{\partial p_i}\frac{\partial f_n}{\partial p_j} w_n \quad ; \quad b_i = \sum_{n=1}^{N} \frac{\partial f_n}{\partial p_i}\left(f_n - y_n\right) w_n \quad ; \quad w_n = \frac{1}{\Delta y_n}$$

A χ^2 merit function is used to assess the goodness of fit and the error in any modelled quantity (e.g. tritium density, diffusion coefficient etc.) can also be obtained:

$$\chi^2 = \sum_{n=1}^{N} w_n \left(y_n - f_n\right)^2 \quad ; \quad \Delta f_n = \sqrt{\sum_{i=1}^{P}\sum_{j=1}^{P} \frac{\partial f_n}{\partial p_i}\frac{\partial f_n}{\partial p_j} M_{ij}^{-1}}$$

With the addition of correlated errors (e.g. relative calibration of the detector system, errors in the influx model and uncertainty in the equilibrium reconstruction) the definition of M becomes

$$M_{ij} = \sum_{m=1}^{N}\sum_{n=1}^{N} w_{n,m}\frac{\partial f_n}{\partial p_i}\frac{\partial f_m}{\partial p_j} \quad ; \quad W = S^{-1} \quad ; \quad s_{n,m} = \rho_{n,m}\sigma_n\sigma_m$$

5 Results for shot 61161

The experiment consisted of two shots, 61158 which was a beam blip experiment and 61161 which was a tritium puff (at $t = 10.5\mathrm{s}$) of around 1% of the total plasma content. Both shots were set up to be similar hybrid-scenario plasmas. A decay time of $\tau = 0.21\mathrm{s}$ was measured from the beam blip shot and used to constrain the transport analysis of shot 61161.

D and v were assumed constant in time for the purposes of the fit. The profiles were fitted as a series of regions (with no discontinuity allowed at boundaries) which were piecewise linear between $r/a = \{0.25, 0.55, 0.7, 0.85\}$. D was kept constant for $r/a < 0.25$ and v was interpolated to 0 from $r/a = 0.25$ to $r/a = 0$. The results are shown in figures 2(a) and 2(b). The measured D and v profiles are not neoclassical as also illustrated in the figures.

Comparisons of the model with the JET neutron profile monitor measurements and global neutron yield are given in figure 3. The r/a given in each plot is representative of the line of sight of each detector. Channels 1–10 are horizontal and channels 11–19 are vertical.

Numerical errors and covariances in free parameters were also obtained from our error analysis procedure, they are shown in tables 1(a) and 1(b). Note that only the strongest covariances (> 0.6) are shown in table 1(b). The global χ^2 for the fit was 1.44.

The key characteristics of D–T neutron emission in the trace tritium pulses are well fitted by UTC[4], thus providing a versatile tool for determining tritium transport.

References

[1] K-D Zastrow *et al*, this conference

[2] K-D Zastrow *et al*, to be published

[3] T Hender *et al*, this conference

[4] A D Whiteford and K-D Zastrow, to be published

[5] S Popovichev *et al*, this conference

[6] M Loughlin *et al* 1999 *Rev. Sci. Instr.* **70** 1126

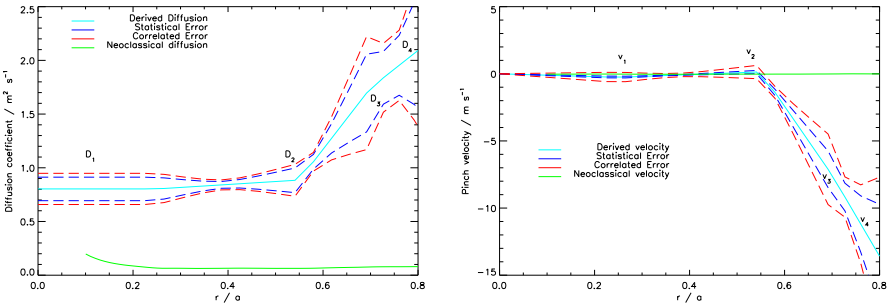

Figure 2: Derived diffusion (a) and convection velocities (b) for shot 61161.

(a)

Param.	Value	Corr.	Uncorr.
D_1	0.80	0.15	0.11
D_2	0.89	0.16	0.12
D_3	1.74	0.56	0.39
D_4	2.27	1.26	0.91
v_1/D_1	-0.33	0.44	0.07
v_2/D_2	0.16	0.60	0.15
v_3/D_3	-4.33	0.92	0.35
v_4/D_4	-7.32	1.66	0.86

(b)

Param. 1	Param 2.	Corr.	Uncorr.
D_1	D_2	-0.82	-0.85
D_2	D_3	-0.74	-0.71
D_3	D_4	-0.77	-0.65
v_1/D_1	v_2/D_2	-0.80	-0.78
v_2/D_2	v_3/D_3	-0.67	-0.17
v_3/D_3	v_4/D_4	-0.87	-0.89
D_1	v_2/D_2	0.66	0.51
D_2	v_2/D_2	-0.58	-0.62

Table 1: Values of parameters & propagated errors (a) and strong covariances (b) in the transport model for both correlated (Corr.) and uncorrelated (Uncorr.) error analysis procedures.

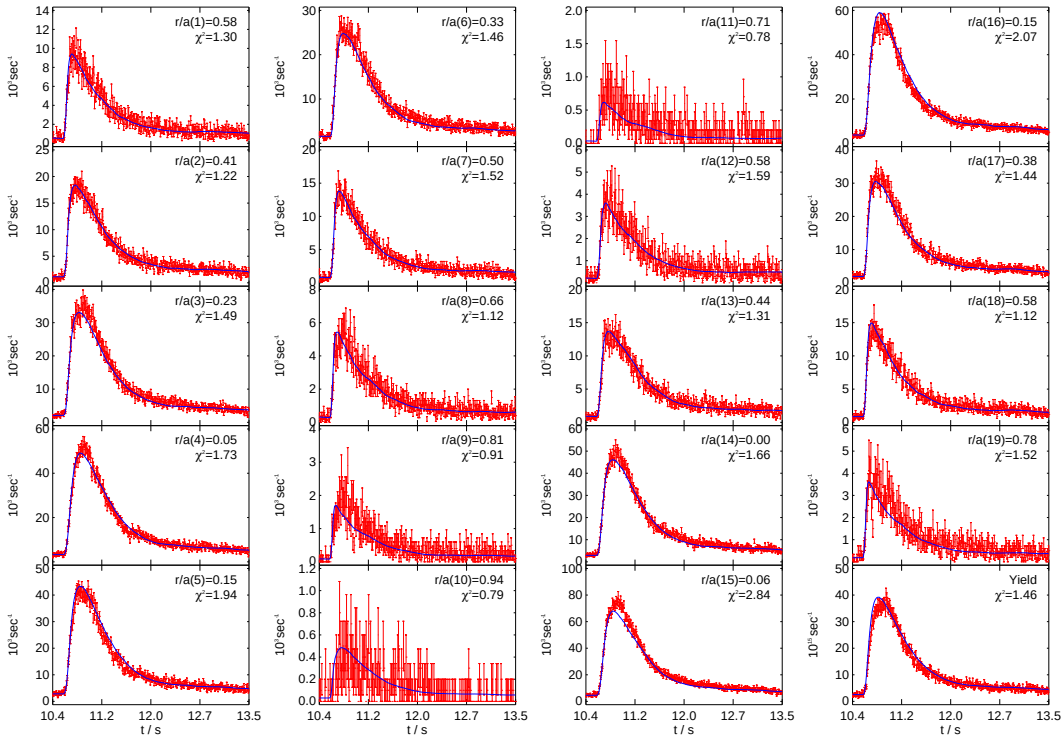

Figure 3: Comparison of modelled (blue) and measured (red) neutron measurements.

Acknowledgements: This work was performed under the European Fusion Development Agreement and partly funded by Euratom and the UK Engineering and Physical Sciences Research Council.